Journal of Applied Geophysics 93 (2013) 43–51

Contents lists available at SciVerse ScienceDirect

Journal of Applied Geophysics

journal homepage: www.elsevier.com/locate/jappgeo

Permeability estimation conditioned to geophysical downhole log data in sandstones of the northern Galilee Basin, Queensland: Methods and application

Zhenjiao Jiang [a,*], Christoph Schrank [a,b], Gregoire Mariethoz [c], Malcolm Cox [a]

[a] School of Earth, Environmental & Biological Sciences, Queensland University of Technology, 4001, QLD, Brisbane, Australia
[b] School of Earth and Environment, The University of Western Australia, 6009, Crawley, WA, Australia
[c] School of Civil and Environmental Engineering, University of New South Wales, UNSW, 2052, Sydney, Australia

ARTICLE INFO

Article history:
Received 17 January 2013
Accepted 17 March 2013
Available online 29 March 2013

Keywords:
Sedimentary basin
Cokriging
Normal linear regression
Bayesian
Permeability
Geophysical logs

ABSTRACT

This study uses borehole geophysical log data of sonic velocity and electrical resistivity to estimate permeability in sandstones in the northern Galilee Basin, Queensland. The prior estimates of permeability are calculated according to the deterministic log–log linear empirical correlations between electrical resistivity and measured permeability. Both negative and positive relationships are influenced by the clay content. The prior estimates of permeability are updated in a Bayesian framework for three boreholes using both the cokriging (CK) method and a normal linear regression (NLR) approach to infer the likelihood function. The results show that the mean permeability estimated from the CK-based Bayesian method is in better agreement with the measured permeability when a fairly apparent linear relationship exists between the logarithm of permeability and sonic velocity. In contrast, the NLR-based Bayesian approach gives better estimates of permeability for boreholes where no linear relationship exists between logarithm permeability and sonic velocity.

1. Introduction

Characterization of the heterogeneity of permeability in sandstones is critical for groundwater, oil and gas exploration (De Marsily et al., 2005; Zimmerman et al., 1998). Many techniques were developed to measure permeability from microscale to macroscale in both hydrogeology and petroleum engineering, for example, tomography approaches, slug tests or drill stem tests (Al-Raoush and Willson, 2005; Bouwer and Rice, 1976; Bredehoeft, 1965). However, because these methods of direct measurement produce costly and sparse data, only limited information can be obtained in regard to understanding the spatial variability of permeability (Hyndman et al., 2000).

Borehole geophysical techniques provide low-cost means to measure geophysical properties that relate to permeability at a fine scale over broad vertical and horizontal intervals (Cassiani et al., 1998; El Idrysy and De Smedt, 2007; Gloaguen et al., 2001). The geophysical properties commonly used to infer permeability include seismic velocity (Rubin et al., 1992), electrical resistivity (Purvance and Andricevic, 2000), and ground-penetrating radar data (Cunningham, 2004; Gloaguen et al., 2001). Various mathematical approaches were employed to tie geophysical properties to permeability, such as regression analysis (Archie, 1942; Purvance and Andricevic, 2000), cokriging interpolation (Kay and Dimitrakopoulos, 2000), Bayesian inference (Chen et al., 2001), and more recently, coupled hydrogeophysical numerical simulations (Day-Lewis and Singha, 2008; Huisman et al., 2010).

Regression analysis is often used to correlate electrical resistivity with permeability, and a log–log linear relationship between these properties can in certain cases be validated theoretically and empirically (Archie, 1942; Purvance and Andricevic, 2000; Wong et al., 1984). This method is efficient, but the relationship between permeability and resistivity is possibly non-unique and ambiguous due to multiple contributing factors, for example, water saturation and clay content, and also possible scale and resolution disparity between the measurements of permeability and resistivity (Ezzedine et al., 1999). As a consequence, other approaches such as Bayesian and cokriging methods are often applied to revise the estimates of permeability.

The Bayesian technique updates the prior estimates of permeability via a likelihood function. The prior estimates of permeability can be obtained from hydrogeologic inversion (Copty et al., 1993) or ordinary kriging interpolation (Shlomi and Michalak, 2007). The likelihood function plays a key role in the Bayesian technique, which can be derived by, for example, ensemble Kalman filter (Evensen, 1994), generalized likelihood uncertainty estimation (Beven and Binley, 1992), or a normal regression model (Chen et al., 2001).

* Corresponding author.
E-mail addresses: jiangzhenjiao@hotmail.com (Z. Jiang), christoph.schrank@qut.edu.au (C. Schrank).

0926-9851/$ – see front matter © 2013 Elsevier B.V. All rights reserved.
http://dx.doi.org/10.1016/j.jappgeo.2013.03.008

In addition, Cokriging (CK) is a method for the linear estimation of vector random functions that considers spatial and inter-variable correlation (Myers, 1985). The CK method can be applied to estimate permeability from geophysical measurements, where the geophysical measurements are considered as a secondary variable (Ahmed et al., 1988). A simple cokriging estimator is expressed by:

$$Z_1 - \mu_1 = \sum_{i=1}^{T} \sum_{\alpha_i}^{n_i} \lambda_{\alpha_i} \left(Z_i\left(x_{\alpha_i}\right) - \mu_i \right), \quad (1)$$

where Z_i is the permeability and the geophysical variables related to the permeability, μ_i is the stationary mean of variable i, and λ_{α_i} is the weight of variable Z_i at x_{α_i} (Goovaerts, 1997). These weights can be obtained from a matrix, which is composed of covariance functions. Therefore, inference of covariance functions from the actual measurements is at the foundation of the CK method.

Another approach to estimating permeability (or hydraulic conductivity) is the coupled hydro-geophysical simulation. The basic steps of this simulation are outlined as follows: (1) prior estimates of hydraulic parameters (permeability); (2) calculation of the hydraulic variables, e.g. water saturation or salinity using fluid flow and solute transport simulation; (3) revision of the geohydrologic environments to forward geophysical properties, typically electrical resistivity; and (4) recalculation of permeability considering geophysical properties, and using them as the new input to the hydrogeologic model. These steps are repeated until both the hydrogeologic and geophysical measurements fit well with the calculated results (Day-Lewis et al., 2003; Hinnell et al., 2010; Kowalsky et al., 2011; Pollock and Cirpka, 2012).

The accuracy of permeability estimated by the above methods depends on the sufficiency of actual permeability measurements. In order to overcome the problem of under-sampling in this study, the CK method is coupled with a Bayesian framework to calculate the likelihood function. Both sonic and electrical log data are used to infer the permeability in this coupled method, assuming that the covariances of permeability and the resistivity are the same.

This study initially introduces the geology of the northern Galilee Basin, followed by a description of Bayesian framework and cokriging theory. The coupled CK–Bayesian method is then tested on three boreholes in the northern Galilee Basin (Fig. 1). The performance of the CK–Bayesian method is compared with another deterministic Bayesian method based on normal linear regression. Finally, the main results are discussed.

2. Study area and data description

2.1. General geological setting

The Galilee Basin is a large intracratonic basin of the Late Carboniferous to Triassic period located in central Queensland, Australia (Fig. 1a). Sediments of the northern Galilee Basin were deposited in two regional depressions, the Koburra Trough and Lovelle Depression,

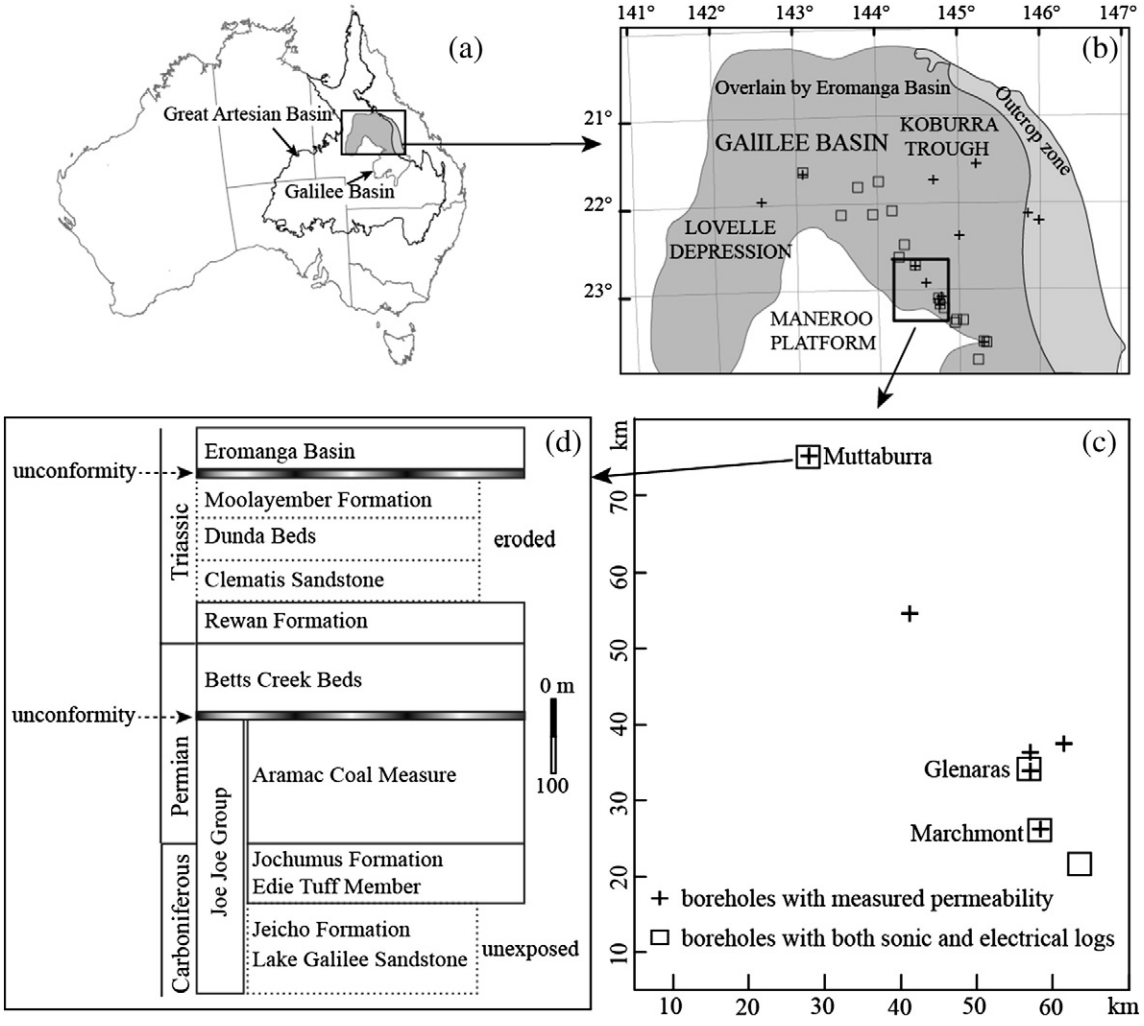

Fig. 1. Location map showing (a) the study area within the northern Galilee Basin, (b, c) boreholes with geophysical logs and permeability measurements, and (d) a schematic column showing the general stratigraphy in the northern Galilee Basin.

which are separated by the early Palaeozoic Maneroo Platform (Fig. 1b) (Hawkins and Green, 1993).

During the Late Carboniferous and Early Permian period, sediments of the Joe Joe Group were deposited by rivers and lakes and were significantly affected by climatic variations and intermittent volcanic activity (Fig. 1d). During the latter part of the Early Permian, development of widespread peat swamps resulted in deposition of the Aramac Coal Measures at the top of Joe Joe Group (Henderson and Stephenson, 1980).

After a period of non-deposition, gentle uplifting and erosion, the Betts Creek Beds were deposited in alluvial, coastal-plain settings during the Late Permian period (Allen and Fielding, 2007).

During the Early to Middle Triassic period, the westerly and southerly flowing rivers and intermittent lakes resulted in the deposition of sandstones and shales of the Rewan Formation and Clematis Sandstone on the Betts Creek Beds. Further deposition produced the Moolayember Formation which is composed of siltstones and mudstones and forms the uppermost formation within the Galilee Basin (Fig. 1d). However, a substantial part of Moolayember Formation was removed in a compressional episode before it was overlain by sediments of the Eromanga Basin (Hawkins and Green, 1993).

The lithology of the study area (Fig. 1c) is dominated by interbedded sandstones and shales, which were deposited by cyclic of fluvial systems. All these formations were deposited in a stable geologic period, except for the earlier Joe Joe Group, which experienced glacial and volcanic activity. Therefore, on the basis of sedimentary facies, the formations in this northern Galilee Basin are separated into an upper part that includes the Betts Creek Beds, Rewan Formation, Clematis Group, Dunda Beds and Moolayember Formation, and a lower part that is comprised of the Joe Joe Group (Fig. 1d). In order to validate the proposed cokriging–Bayesian method, this study concentrates on the upper formations where the permeability of sandstones was tested and geophysical logs of sonic velocity and electrical resistivity are available.

2.2. Data analysis and pre-processing

The geophysical log data supporting this study are from the Queensland Petroleum Exploration Database (QPED, http://mines.industry.qld.gov.au/geoscience/geoscience-wireline-log-data.htm) and Exoma Energy Ltd. Both the sonic velocity (measured by borehole sonic logs) and electrical resistivity (acquired by borehole electrical logs) are correlated with permeability in this deep buried basin. However, the relationship between these parameters can be ambiguous due to the effects of variable clay contents (Friedel et al., 2006). In addition, permeability of shale is too low ($<10^{-3}$ mD) to be estimated accurately from geophysical log data.

In order to reduce the impact of clay, shales are identified and removed from this study by a qualitative interpretation of geophysical log data. Electrical and gamma ray log data are used for this purpose because shales often display lower electrical resistivity but higher gamma radiation than sandstones (Kayal, 1979). In addition, spontaneous potential logs which can show the interface between different lithologies, are also used (Wood et al., 2003). Fig. 2 illustrates the interpreted results in the Muttaburra borehole as an example.

After the approximate identification of shales from geophysical logs, clay contents in sandstones are computed by the following empirical equations (Mahbaz et al., 2012):

$$I_{GR} = \frac{GR_{\log} - GR_{\min}}{GR_{\max} - GR_{\min}}, \tag{2}$$

$$S_c = \begin{cases} 0.0006078(100I_{GR})^{1.58257} & I_{GR}<0.55 \\ 2.1212I_{GR}-0.81667 & 0.73 > I_{GR} > 0.55 \\ I_{GR} & I_{GR} > 0.73 \end{cases}, \tag{3}$$

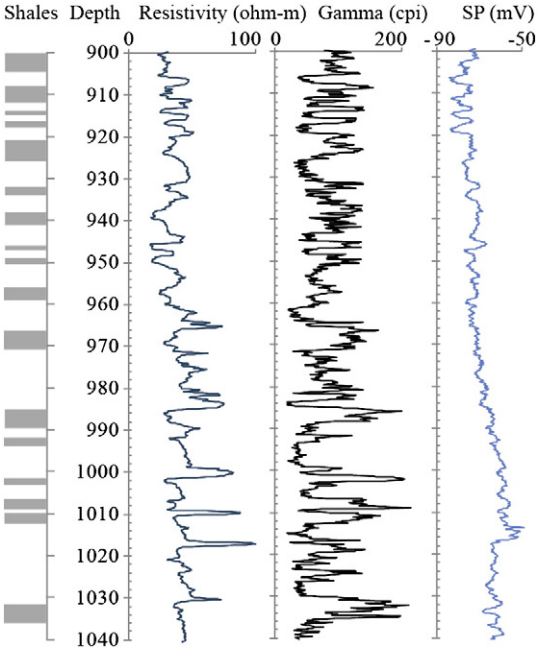

Fig. 2. Shales (grey rectangle) identified according to geophysical logs of natural gamma, deep resistivity and spontaneous potential (SP) in Muttaburra.

where I_{GR} is a gamma ray index, $GR_{\log}$ is gamma radiation, $GR_{\min}$ and $GR_{\max}$ are maximum and minimum gamma radiation, respectively. S_c is the clay content. The results from Eqs. (2) and (3) are used in Section 4.1 to establish the empirical relationship between electrical resistivity and permeability.

Comparison of the histograms of Fig. 3a and b shows that the removal of shale reduces the "smearing effect" in the probability distribution of sonic velocity. Importantly, the histogram of electrical resistivity changes from bimodal to quasi-Gaussian if shales are disregarded (Fig. 3c and d). The distributions of electrical resistivity and sonic velocity are slightly skewed in sandstone because the measurements are affected by the surrounding shale.

Based on the histograms shown in Fig. 3, it is reasonable to assume a Gaussian probability density function (PDF) once the shale is identified and removed. The Gaussian PDF is widely used in many geostatistical methods, and is formulated as:

$$p = \frac{1}{\sqrt{2\pi\sigma^2}} e^{-\frac{|Z(x)-\mu|^2}{2\sigma^2}}, \tag{4}$$

where p is the probability density, σ^2 is the variance and μ is the mean of variable Z.

3. Methodology

3.1. Bayesian framework

In this study, the Bayesian methodology is used to estimate permeability from correlated geophysical log data. The spatial random variable $k(x)$ denotes $\log_{10}$ of permeability (mD), $DT(x)$ denotes sonic velocity (ms/feet), and $\rho(x)$ denotes electrical resistivity (ohm-m). According to Bayes' rule, the posterior PDF of permeability given sonic velocity is written as (Lee, 2012; Mariethoz et al., 2010):

$$p(k|DT) = C \cdot p(DT|k) \cdot p(k), \tag{5}$$

where C is a normalizing coefficient, $p(DT|k)$ is the likelihood which is the probability density of sonic velocity given the permeability, and $p(k)$ is the prior PDF of $k(x)$.

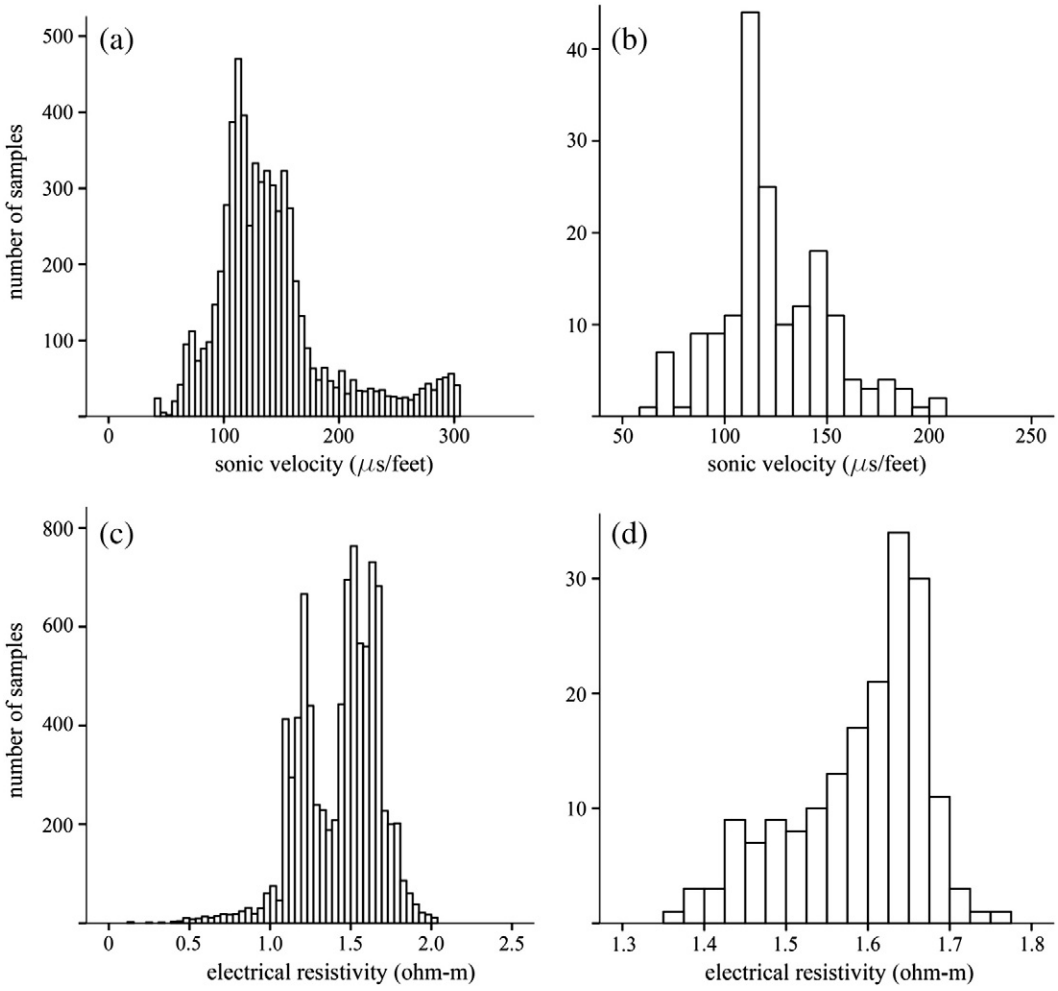

Fig. 3. Histograms of (a) sonic velocity and (c) $\log_{10}$-electrical resistivity measured in shales and sandstones in Muttaburra borehole at a separation of 0.2 m, (b) sonic velocity and (d) $\log_{10}$-electrical resistivity measured in sandstones at an average separation of 1.0 m.

Since, by definition, $\int_0^\infty p(k|DT)dk = 1$, C can be calculated by

$$C = \frac{1}{\int_0^\infty p(DT|k)\cdot p(k)dk}. \tag{6}$$

The prior distribution of k is commonly estimated using an ordinary kriging approach based on the actual permeability measurements (Ezzedine et al., 1999; Shlomi and Michalak, 2007). However, the number of actual permeability measurements in this study is not sufficient to quantify the covariance of permeability. Consequently, k cannot be inferred by the ordinary kriging method. Alternatively, the prior estimates of permeability are calculated according to the empirical relationship between measured electrical resistivity and permeability. The details of this procedure are described in Sections 4.1 and 4.3.

The likelihood in Eq. (5) is assumed to follow a Gaussian distribution (Eq. (4)). In this study, we use the cokriging method (CK) to calculate the mean and variance of the likelihood. In order to validate the effectiveness of the CK-based Bayesian method, the approach is compared with a normal linear regression (NLR) method for the calculation of the likelihood.

3.2. Cokriging model

The CK algorithm considers the mean of likelihood at location x_i as the linear combination of first attributes $DT(x)$ and second attributes $k(x)$. All sonic velocity and prior estimates of permeability used are mean-removed and normalized by their global standard deviation. This linear estimator of likelihood at x_i can be written as (Goovaerts, 1997):

$$\mu(x_i) = \sum_{\substack{j=1\\ j\neq i}}^{n_1} \lambda_{1j}(x_i) DT\left(x_j\right) + \sum_{j=1}^{n_2} \lambda_{2j}(x_i) k\left(x_j\right), \tag{7}$$

where, n_1 and n_2 are the number of DT and k measurements, respectively. λ_{1j} and λ_{2j} are the weighting coefficients of DT and k measurements at location x_j. Because Eq. (7) is used to estimate the mean of likelihood, it is allowed to be a biased estimator.

By minimizing the local variance at x_i,

$$\min : \sigma^2(x_i) = E[\mu(x_i) - DT(x_i)]^2, \tag{8}$$

where E denotes the mean operator. Subsequently, the coefficients λ at location x_i can be solved from the following equations:

$$\begin{aligned}
&\sum_{\substack{w_1=1\\ w_1\neq i}}^{n_1} \lambda_{1w_1}(x_i) C_{11}\left(x_{v_1} - x_{w_1}\right) + \sum_{w_2=1}^{n_2} \lambda_{2w_2}(x_i) C_{12}\left(x_{v_1} - x_{w_2}\right) \\
&\quad = C_{11}\left(x_{v_1} - x_i\right), v_1 = 1, ..i-1, i+1..n_1 \\
&\sum_{\substack{w_1=1\\ w_1\neq i}}^{n_1} \lambda_{1w_1}(x_i) C_{21}\left(x_{v_2} - x_{w_1}\right) + \sum_{w_2=1}^{n_2} \lambda_{2w_2}(x_i) C_{22}\left(x_{v_2} - x_{w_2}\right) \\
&\quad = C_{21}\left(x_{v_2} - x_i\right), v_2 = 1, ..n_2
\end{aligned} \tag{9}$$

where C_{ii} and C_{ij} are the pseudo auto- and cross-covariance function expressed by, for example, $C_{ij}(x_1 - x_2) = E[DT(x_1)]E(k[(x_2)]$ without removing the local mean of sonic velocity and permeability at x_1 and x_2.

The variance of likelihood at location x_i is expressed by:

$$\sigma^2(x_i) = C_{11}(0) - \sum_{\substack{w_1=1 \\ w_1 \neq i}}^{n_1} \lambda_{1w_1}(x_i) C_{11}\left(x_{w_1} - x_i\right) - \sum_{w_2=1}^{n_2} \lambda_{2w_2}(x_i) C_{21}\left(x_{w_2} - x_i\right). \tag{10}$$

The stationary assumption is used, which assumes that the pseudo-covariance only depends on the separation (x_1–x_2) between two points, but not their locations. Since this assumption is also used in the standard cokriging approach (Goovaerts, 1997), the cokriging method used here is achieved in a similar way to the standard approach. Hereafter, we still use the terms of "auto-covariance" and "cross- covariance" to express the structural functions.

Eq. (8) minimizes the local variance. In order to further maximize the likelihood, the covariance models are adjusted artificially to minimize the global error:

$$error = \frac{1}{n_1} \sum_{i=1}^{n_1} [\mu(x_i) - DT(x_i)]^2 \ , \tag{11}$$

3.3. Normal linear regression model

The NLR model assumes that sonic velocity at x is normally distributed with mean $\mu(x)$ and variance σ^2 (Chen et al., 2001; Stone, 1996). The mean of likelihood is assumed to be the sum of m distinct monomials, formed from powered products of $k(x)$, such as 1, $k(x)$, $k^2(x)$,… $k^{m-1}(x)$. The model is expressed as follows:

$$\mu(x) = \sum_{i=1}^{m} \beta_i k^{i-1}(x), \tag{12}$$

where β_i is the weighting coefficient of basic functions $k^{i-1}(x)$.

By minimizing the residual variances (Chen et al., 2001),

$$RSS = \sum_{j=1}^{n} \left[DT\left(x_j\right) - \mu\left(x_j\right)\right]^2, \tag{13}$$

the weighting coefficients is obtained as:

$$\boldsymbol{\beta} = \left(\mathbf{D}^T\mathbf{D}\right)^{-1}\mathbf{D}^T\mathbf{Z}, \tag{14}$$

using a matrix notation where $\boldsymbol{\beta} = (\beta_1, \beta_2 \ldots \beta_m)^T$, $\mathbf{Z} = [DT(x_1) \ldots DT(x_n)]^T$, and n is the number of locations where both sonic velocity and permeability are measured. $\mathbf{D}$ is a $n \times$ m synthetic matrix given by,

$$\mathbf{D} = \begin{bmatrix} 1 & k(x_1) & k^2(x_1) & \ldots & k^{m-1}(x_1) \\ 1 & k(x_2) & k^2(x_2) & \ldots & k^{m-1}(x_2) \\ \ldots & & \ldots & & \ldots \\ 1 & k(x_n) & k^2(x_n) & \ldots & k^{m-1}(x_n) \end{bmatrix}, \tag{15}$$

Once the basic coefficients are determined, the mean likelihood at each location is calculated by Eq. (12).

The variance of likelihood is expressed by:

$$\sigma^2 = \frac{1}{n-m} \sum_{j=1}^{n} \left[DT\left(x_j\right) - \mu\left(x_j\right)\right]^2. \tag{16}$$

3.4. The theoretical differences between CK and NLR-based Bayesian method

Both approaches assume a Gaussian PDF for the prior, likelihood and posterior probability. However, the CK and NLR approaches consider the parameters in these distributions differently, which are summarized in Table 1. The "local" represents a statistical process at given depth, while the term "global" denotes statistical measures obtained from data at different depths.

3.4.1. Prior estimates

The NLR–Bayesian method uses the prior estimates of permeability as the local mean $\mu(x_i)$ at x_i, and uses the global variance of permeabilities in the prior PDF. The global variance is defined as:

$$\sigma^2 = \frac{1}{n} \sum_{i=1}^{n} [k(x_i) - \mu]^2 \ , \tag{17}$$

where n is number of the actual permeabilities measurements at different depths in a borehole, μ is a global mean of prior estimates which are calculated by:

$$\mu = \frac{1}{n} \sum_{i=1}^{n} k(x_i) \ , \tag{18}$$

In contrast, the CK–Bayesian method uses both global mean and variance (Eqs. (17) and (18)) in the prior PDF of permeability. However, n is the number of the prior estimates of permeability but not that of the actual permeability measurements. The prior PDF in CK–Bayesian approach is conditional, $p[k(x_i)|k(x_1) \ldots k(x_{i-1}), k(x_{i+1}) .. k(x_m)]$, while the prior PDF in the NLR–Bayesian approach is marginal, $p[k(x_i)]$.

3.4.2. Likelihood function

The NLR–Bayesian method considers the mean of the likelihood as a local value (Eq. (12)) but the variance as a global one (Eq. (16)). The PDF for the likelihood is expressed by $p[DT(x_i)|k(x_i)]$.

However, both mean and variance of likelihood in the CK–Bayesian method are local, and are expressed by Eqs. (7) and (10), respectively. The PDF of the likelihood is conditional: $p[DT(x_i)|DT(x_1) \ldots DT(x_{i-1}), DT(x_{i+1}), \ldots DT(x_m), k(x_1) \ldots k(x_m)]$.

3.4.3. Posterior estimates

Both NLR– and CK–Bayesian methods express the mean and variance of posterior estimates at a given depth as a local statistical variable, but with different conditional probability densities, which are $p[k(x_i)|DT(x_i)]$ for NRL and $p[k(x_i)|DT(x_1) \ldots DT(x_m), k(x_1) \ldots k(x_{i-1}), k(x_{i+1}) .. k(x_m)]$ for CK, respectively.

4. Hydraulic conductivity estimation

In order to validate the CK–Bayesian approach, we use data from the three boreholes, Marchmont, Muttaburra and Glenaras (Fig. 1c), where both sonic and electrical logs were run, and permeabilities were tested by drill stem test (DST) and laboratory measurements using permeameter (data from QPED). The permeabilities determined

Table 1
The mean and variance of prior, likelihood and posterior probability distribution in the normal linear regression and cokriging Bayesian estimator.

Estimator	NLR Bayesian estimator			CK Bayesian estimator		
Probability	Prior	Likelihood	Posterior	Prior	Likelihood	Posterior
Mean	Local	Local	Local	Global	Local	Local
Variance	Global	Global	Local	Global	Local	Local

from the geophysical data are calculated at a length scale of 1.0 m. The length scale of DST is around 0.5–2.0 m and that of cores ranges from 0.1 to 0.5 m. Because these length scales are similar, permeabilities determined from these different methods are comparable. The effectiveness of the CK–Bayesian method is also compared with NLR–Bayesian method.

Permeability estimation with the CK– and NLR–Bayesian methods entails the following steps: (1) estimation of prior PDF of permeability based on the electrical resistivity log data; (2) calculation of the likelihood function using both the CK and NRL methods, respectively, where the likelihood function is the probability of permeability conditioned to the sonic log data; and (3) the posterior estimation of permeability based on Bayes' theorem in Eq. (5).

4.1. Prior estimation

Prior estimates of the permeability in sandstones are converted from geoelectrical log data based on an experimental relationship. This relationship is established by mapping the measured permeability versus electrical resistivity measured at the same location. Fig. 4 illustrates that permeability (k) as a function of electrical resistivity (ρ) is affected by the clay content in upper formations of the north Galilee Basin. A negative correlation is observed between $\log(k)$ and $\log(\rho)$ when the clay content is less than 5%; conversely, a positive correlation is obtained when the clay content is greater than 5%.

The electrical resistivity of earth materials relates to electrolytes in the pore fluid and electrons on the pore surface (Niwas and Singhal, 1985). In clay-free sandstone, the electrical current is dominated by electrical conduction through the pore fluid. An increase in porosity leads to an increase in permeability and thus to a decrease in electrical resistivity (Slater, 2007). Therefore, a negative trend is observed between ρ and k when no significant clay content is present.

However, in clay-rich sandstones, electrical current is controlled by electrical conduction on pore surfaces (Purvance and Andricevic, 2000). Permeability commonly decreases with an increase in clay content. The same trend exists between electrical resistivity and clay content when clay content is larger than 5%. Therefore, a positive relationship between ρ and k is observed in clay-rich sandstones.

Based on the plots in Fig. 4, a bilinear experimental petrophysical equation is given for sandstone formations in the northern Galilee Basin:

$$\log k(x) = \begin{cases} -6.3753\log\rho(x) + 13.066 & S_c < 5\% \\ 1.8711\log\rho(x) - 2.5992 & S_c > 5\% \end{cases}, \quad (19)$$

Although the permeability can be estimated from this bilinear relationship, the low correlation coefficients (0.4091 and 0.3033, respectively) indicate large estimation errors. Therefore, the permeability estimated from this empirical equation is considered as prior estimate only. These results are then updated and improved via the Bayesian framework.

Table 2
The coefficients to calculate the likelihood functions.

Boreholes	β_1	β_2	β_3	β_4	β_5	β_6
Marchmont	0.9754	1.2007	1.5734	0	0	0
Muttaburra	−1.5406	3.8752	−1.7358	0.0335	0	0
Glenaras	0.5271	−0.3883	−2.0932	3.5008	−1.76532	0.2794

4.2. Updating by Bayesian statistics

4.2.1. NLR-based estimation

The likelihood function plays a central role in Bayesian methods. In the NLR approach, the mean and variance of the likelihood are determined by the coefficients of basic functions, which can be calculated by Eq. (14) based on the actual measurements of permeability and sonic velocity. There are five such actual measurements in Marchmont borehole, six in Muttaburra and seven in Glenaras boreholes. In a single borehole, these coefficients are considered to be spatially stationary at different depths. The resulting coefficients for each borehole are shown in Table 2.

Once these coefficients are obtained, the mean and variance of the likelihood at different depths are estimated by Eqs. (12) and (16), respectively. Consequently, the Gaussian PDF of the likelihood is quantified by Eq. (4). Finally, the posterior estimates of permeability are obtained by Eq. (5) and results are shown in Fig. 5a and c.

4.2.2. CK-based estimation

The CK approach assesses the mean and variance of the likelihood based on structural functions: auto- and cross- covariance. In this study, the covariance of permeability is assumed to be the same as the covariance of electrical resistivity after both are logarithm-transformed, mean-removed and normalized. This assumption is satisfied in this study because electrical resistivity and permeability are correlated linearly in each borehole (Fig. 4 and Eq. (19)). Therefore, the covariance of prior estimates of permeability can be used to infer the likelihood via the CK algorithm. The covariances of the prior estimates of permeability and sonic velocity at different separations (from 0 to 1000 m) are calculated and fitted using a spherical covariance model using the Matlab code *variogramfit* (Minasny and McBratney, 2005).

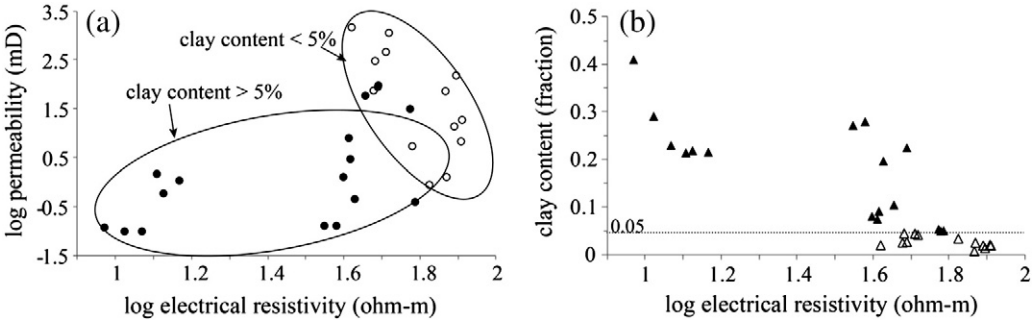

Fig. 4. Scatterplots of (a) negative and positive linear relationships between $\log_{10}$-electrical resistivity and $\log_{10}$-permeability relating to clay content, and (b) negative relationship between $\log_{10}$-electrical resistivity and clay content when clay content is larger than 5%. Raw data are extracted from the Queensland Petroleum Exploration Database.

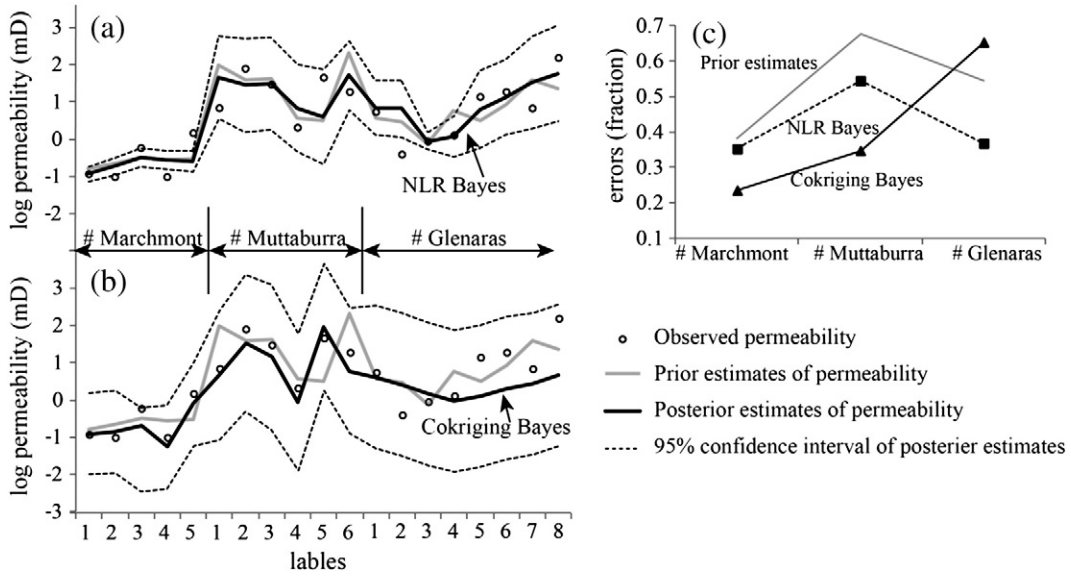

Fig. 5. Estimates of permeability from (a) normal linear regression and (b) cokriging Bayesian approaches, (c) the mean estimate-errors of different methods, $E(|k_e - k_m|)$, where k_e is the estimated permeability and k_m is the measured permeability.

Below, the Muttaburra data is used as an example to show the CK–Bayesian approach. The general expressions of the spherical model used in Muttaburra borehole are written as follows:

$$C_{ii}(h) = \begin{cases} 1 \quad if \ \ h = 0 \\ 1 - nug - s\cdot\left[1.5\left(\frac{|h|}{a}\right) - 0.5\left(\frac{|h|}{a}\right)^3\right] \quad if \ \ 0 < |h| \le a \\ 0 \quad if |h| > a \end{cases} \quad , \qquad (20)$$

$$C_{ij}(h) = \begin{cases} -0.45 \quad if \ \ h = 0 \\ nug + s\cdot\left[1.5\left(\frac{h}{a}\right) - 0.5\left(\frac{h}{a}\right)^3\right] - 0.45 \quad if \ \ 0 < |h| \le a \\ 0 \quad if |h| > a \end{cases} \quad , \qquad (21)$$

where, $C_{ii}(h)$ is the auto-covariance of prior permeability and sonic velocity, $C_{ij}(h)(i \neq j)$ is the cross-covariance between permeability and sonic velocity, h is separation, *nug* is the nugget value which is introduced by the measurement errors, s is the sill, and a is the correlation range.

In the models above (Fig. 6), the cross-covariance is asymmetric ($C_{ij}(h) \neq C_{ij}(-h)$), and a negative correlation is obtained between sonic velocity and permeability. Due to the cyclicity of lithology in the Galilee Basin, a large covariance may arise when the separation (h) becomes larger than a. Therefore, in this study the covariance is set to zero when the separation is larger than a.

The constants (*nug*, s and a) are inferred by cross-validation, which removes one point in the data series and calculates its value using the others to minimize calculation errors in Eq. (11) (Haberlandt, 2007). One advantage of coupling the CK method with a Bayesian framework is that the covariance function can be adjusted based on the dense measurements of sonic velocity instead of sparse permeability measurements used in the direct CK method. The purpose of the adjustment of constants here is not to find the unbiased estimates of sonic velocity, but to maximize the likelihood. Therefore, biased estimates of sonic velocity are allowed in CK in the Bayesian framework.

Once the covariance functions are determined, the local mean and variance of the likelihood can be calculated by Eqs. (7) and (10), respectively. Subsequently, the posterior estimates of permeability are obtained by Eq. (5). The results are displayed in Fig. 5b and c.

4.3. Discussion

The NLR-based Bayesian method systematically yields better estimates of permeability than the prior estimates, with a narrow 95% confidence interval (Fig. 5a) and smaller estimate errors (Fig. 5c). In Marchmont and Glenaras boreholes, however, the confidence interval does not include all actual measurements of permeability. This is because only five to seven actual measured permeabilities are available to assess the means and variances of likelihood in these boreholes. Indeed, in most boreholes in this study area, only geophysical log data are available but no actual permeability measurements (Fig. 1b).

In the absence of the permeability measurements, the CK-based Bayesian method allows for the estimation of permeability from geophysical data, because (a) a global mean is used in the prior PDF, which can decrease the impact of errors in prior estimates at a given location; and (b) local mean and variance are used in the likelihood calculation, and both depend on the covariance of the sonic velocity and the prior estimates of permeability, instead of the actual measurements of permeability.

Fig. 5b and c show that the posterior estimates of permeability by the CK-based Bayesian method are in good agreement with the actual measurements in Marchmont and Muttaburra boreholes. The errors are smaller than those of prior estimates and the NLR-based Bayesian method.

However, there is no linear relationship between sonic velocity and permeability in Glenaras borehole (Fig. 7b). Consequently, the cross-covariance function cannot be modelled appropriately, and CK-based Bayesian approach fails to estimate permeability in the Glenaras borehole properly (Fig. 5a and c). This result indicates that CK-based Bayesian approach requires an apparent linear relationship between sonic velocity and permeability to model the covariance function (Fig. 7a and c).

The discussions above suggest merits of both NLR– and CK–Bayesian approaches. They infer the likelihood differently. The NLR–Bayesian approach is a point to point estimator, where the likelihood function is determined by a group of coefficients (β in Eq. (12)). The advantage of the NLR-based method is that the sonic velocity is considered as a combination of permeability at different orders. Therefore, this method can characterize the likelihood in the Glenaras borehole where no linear relationship is shown between permeability and sonic velocity.

The CK-based method, in contrast, employs structural functions, and considers the mean of the likelihood as a linear combination of

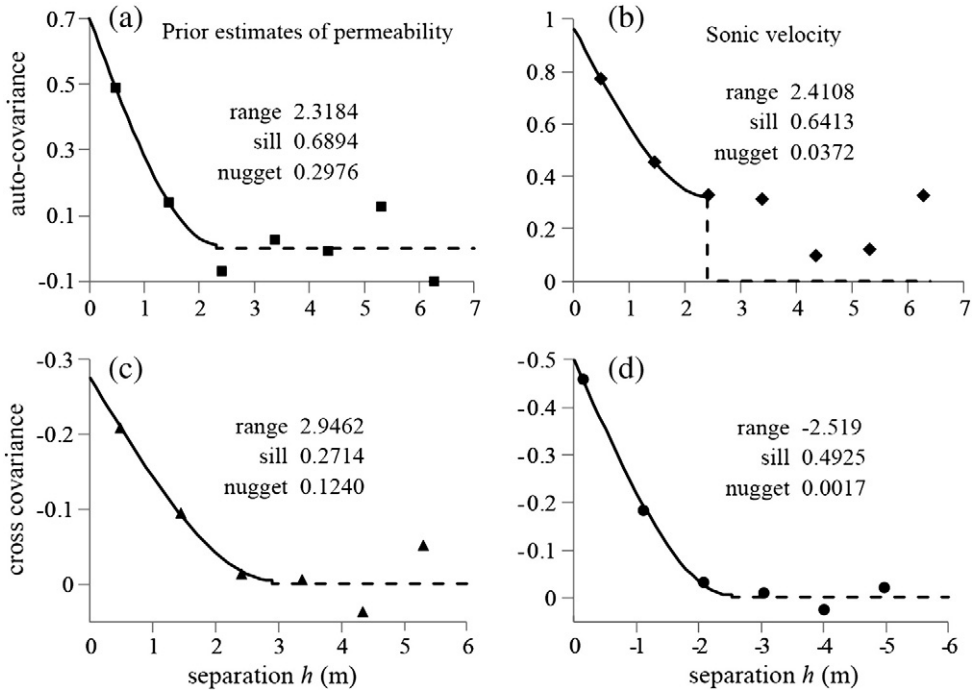

Fig. 6. Experimental and modeled auto- and cross-covariance functions in Muttaburra borehole. The functions are fitted using a spherical model. (a) Auto-covariance of prior estimates of permeability, which is the same as that of electrical resistivity; (b) auto-covariance of sonic velocity; (c) and (d) display the cross-covariance between electrical resistivity and sonic velocity at the separation of h and $-h$, respectively. Note that $C_{ij}(h) = C_{ij}(-h)$.

spatial variables adjacent to the estimated location. The advantage of this approach is that it considers the spatial correlation of the measured data. This is important when applying geophysical data, because a geophysical measurement at one location is generally an average property of, or affected by, the physical properties of adjacent locations. Therefore, when the structural functions (covariances) can be determined, the CK-based method can yield better estimates of permeability.

In future work, the CK-based Bayesian method will be used to estimate permeability in another 18 boreholes in the northern Galilee Basin (Fig. 1b), where no permeability was measured. The heterogeneity of permeability in this basin will be better understood after

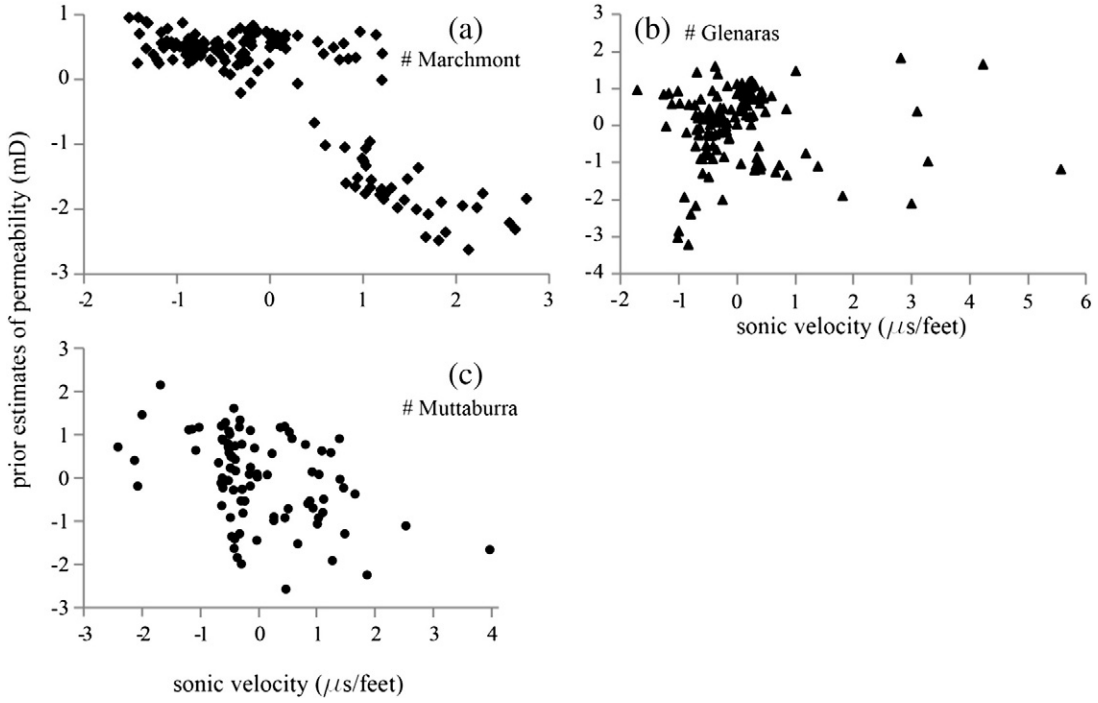

Fig. 7. Scatterplots of prior estimates of the permeability and sonic velocity in (a) Marchmont, (b) Glenaras and (c) Muttaburra boreholes. Both permeability and sonic velocity are mean-removed and normalized. A weak negative correlation is shown in Marchmont and Muttaburra boreholes, but no clear linear correlation is displayed in Glenaras borehole.

the permeability is calculated at a separation of 1.0 m in each borehole.

5. Conclusion

This study introduces a new method, which couples the cokriging (CK) with the Bayesian framework to estimate the permeability from geophysical log data (electrical resistivity and sonic velocity). The method can be applied even without actual measurements of permeability, provided that the covariances of electrical resistivity and permeability are the same in sandstones measured.

In this approach, the prior estimates of permeability are assessed from an experimental log–log linear relationship between permeability and electrical resistivity in three boreholes: Marchmont, Muttaburra and Glenaras. The likelihood is assumed to be described by a Gaussian PDF. The mean and variance of the likelihood are determined by cokriging using sonic velocity as the first covariate and prior estimates of permeability as the secondary covariate.

The results of the CK-based Bayesian method are compared with the actual measurements of permeability and another Bayesian method, which calculates the likelihood by a normal linear regression (NLR) method. The results show that the NLR-based Bayesian method always improves the prior estimates of permeability in the three boreholes studied, but the number of the actual permeability measurements of permeability restricts output quality. The CK-based Bayesian method significantly improves the prior estimates of permeability and yields good agreement with the actual measurements in Marchmont and Muttaburra boreholes. However, the CK-based Bayesian method fails to estimate the permeability in Glenaras because no linear relationship exists between permeability and sonic velocity, hence the covariance between them cannot be well determined.

In summary, the CK-based Bayesian method is an effective approach to inferring permeability from geophysical log data even in situations without actual permeability measurement.

Acknowledgments

Funding support for this study came from China Scholarship Council, and financial support from Exoma Energy Ltd. is also gratefully acknowledged. Daniel Owen is thanked for input to the article structure, and Dr. Oliver Gaede for helpful discussions. Professor Klaus Holliger, Professor Kevin J. Cunningham, and an anonymous reviewer are thanked for their comments on this paper.

References

Ahmed, S., de Marsily, G., Talbot, A., 1988. Combined use of hydraulic and electrical properties of an aquifer in a geostatistical estimation of transmissivity. Ground Water 26 (1), 78–86.
Allen, J.P., Fielding, C.R., 2007. Sedimentology and stratigraphic architecture of the Late Permian Betts Creek Beds, Queensland, Australia. Sedimentary Geology 202 (1–2), 5–34.
Al-Raoush, R.I., Willson, C.S., 2005. Extraction of physically realistic pore network properties from three-dimensional synchrotron X-ray microtomography images of unconsolidated porous media systems. Journal of Hydrology 300 (1–4), 44–64.
Archie, G.E., 1942. The electrical resistivity log as an aid in determining some reservoir characteristics. Transactions of AIME 146, 54–62.
Beven, K., Binley, A., 1992. The future of distributed models: model calibration and uncertainty prediction. Hydrological Processes 6 (3), 279–298.
Bouwer, H., Rice, R.C., 1976. A slug test for determining hydraulic conductivity of unconfined aquifers with completely or partially penetrating wells. Water Resources Research 12 (3), 423–428.
Bredehoeft, J.D., 1965. The drill-stem test: the petroleum industry's deep-well pumping test. Ground Water 3 (3), 31–36.
Cassiani, G., Böhm, G., Vesnaver, A., Nicolich, R., 1998. A geostatistical framework for incorporating seismic tomography auxiliary data into hydraulic conductivity estimation. Journal of Hydrology 206 (1–2), 58–74.
Chen, J., Hubbard, S., Rubin, Y., 2001. Estimating the hydraulic conductivity at the south oyster site from geophysical tomographic data using Bayesian techniques based on the normal linear regression model. Water Resources Research 37 (6), 1603–1613.
Copty, N., Rubin, Y., Mavko, G., 1993. Geophysical–hydrological identification of field permeabilities through Bayesian updating. Water Resources Research 29 (8), 2813–2825.
Cunningham, K.J., 2004. Application of ground-penetrating radar, digital optical borehole images, and cores for characterization of porosity hydraulic conductivity and paleokarst in the Biscayne aquifer, southeastern Florida, USA. Journal of Applied Geophysics 55 (1–2), 61–76.
Day-Lewis, F.D., Singha, K., 2008. Geoelectrical inference of mass transfer parameters using temporal moments. Water Resources Research 44 (5), W05201.
Day-Lewis, F.D., Lane Jr., J.W., Harris, J.M., Gorelick, S.M., 2003. Time-lapse imaging of saline-tracer transport in fractured rock using difference-attenuation radar tomography. Water Resources Research 39 (10), 1290.
De Marsily, G., et al., 2005. Dealing with spatial heterogeneity. Hydrogeology Journal 13 (1), 161–183.
El Idrysy, E.H., De Smedt, F., 2007. A comparative study of hydraulic conductivity estimations using geostatistics. Hydrogeology Journal 15 (3), 459–470.
Evensen, G., 1994. Sequential data assimilation with a nonlinear quasi-geostrophic model using Monte Carlo methods to forecast error statistics. Journal of Geophysical Research 99 (C5), 10143–10162.
Ezzedine, S., Rubin, Y., Chen, J., 1999. Bayesian method for hydrogeological site characterization using borehole and geophysical survey data: Theory and application to the Lawrence Livermore National Laboratory Superfund Site. Water Resources Research 35 (9), 2671–2683.
Friedel, S., Thielen, A., Springman, S.M., 2006. Investigation of a slope endangered by rainfall-induced landslides using 3D resistivity tomography and geotechnical testing. Journal of Applied Geophysics 60 (2), 100–114.
Gloaguen, E., Chouteau, M., Marcotte, D., Chapuis, R., 2001. Estimation of hydraulic conductivity of an unconfined aquifer using cokriging of GPR and hydrostratigraphic data. Journal of Applied Geophysics 47 (2), 135–152.
Goovaerts, P., 1997. Geostatistics for natural resources evaluation. Applied geostatistics series. Oxford University Press, New York (483 pp.).
Haberlandt, U., 2007. Geostatistical interpolation of hourly precipitation from rain gauges and radar for a large-scale extreme rainfall event. Journal of Hydrology 332 (1–2), 144–157.
Hawkins, P., Green, P., 1993. Exploration results, hydrocarbon potential and future strategies for the northern Galilee Basin. The APEA Journal 33, 280–296.
Henderson, R.A., Stephenson, P.J., 1980. The geology and geophysics of northeastern Australia. Geological Society of Australia, Qld. Division 468.
Hinnell, A.C., et al., 2010. Improved extraction of hydrologic information from geophysical data through coupled hydrogeophysical inversion. Water Resources Research 46, W00D40.
Huisman, J.A., Rings, J., Vrugt, J.A., Sorg, J., Vereecken, H., 2010. Hydraulic properties of a model dike from coupled Bayesian and multi-criteria hydrogeophysical inversion. Journal of Hydrology 380 (1–2), 62–73.
Hyndman, D.W., Harris, J.M., Gorelick, S.M., 2000. Inferring the relation between seismic slowness and hydraulic conductivity in heterogeneous aquifers. Water Resources Research 36 (8), 2121–2132.
Kay, M., Dimitrakopoulos, R., 2000. Integrated interpolation methods for geophysical data: applications to mineral exploration. Natural Resources Research 9 (1), 53–64.
Kayal, J.R., 1979. Electrical and gamma-ray logging in Gondwana and tertiary coal fields of India. Geoexploration 17 (3), 243–258.
Kowalsky, M.B., et al., 2011. Coupled modeling of hydrogeochemical and electrical resistivity data for exploring the impact of recharge on subsurface contamination. Water Resources Research 47 (2), W02509.
Lee, P.M., 2012. Bayesian Statistics: An Introduction. Wiley, Hoboken 484.
Mahbaz, S., Sardar, H., Memarian, H., 2012. Determination of a rock physics model for the carbonate Fahliyan Formation in two oil wells in southwestern Iran. Exploration Geophysics 43 (1), 47–57.
Mariethoz, G., Renard, P., Caers, J., 2010. Bayesian inverse problem and optimization with iterative spatial resampling. Water Resources Research 46 (11), W11530.
Minasny, B., McBratney, A.B., 2005. The Matérn function as a general model for soil variograms. Geoderma 128 (3–4), 192–207.
Myers, D.E., 1985. Cokriging: Methods and alternatives. The role of Data in Scientific Progress. Elsevier Scientific Pub., New York.
Niwas, S., Singhal, D.C., 1985. Aquifer transmissivity of porous media from resistivity data. Journal of Hydrology 82 (1–2), 143–153.
Pollock, D., Cirpka, O.A., 2012. Fully coupled hydrogeophysical inversion of a laboratory salt tracer experiment monitored by electrical resistivity tomography. Water Resources Research 48 (1), W01505.
Purvance, D.T., Andricevic, R., 2000. Geoelectric characterization of the hydraulic conductivity field and its spatial structure at variable scales. Water Resources Research 36 (10), 2915–2924.
Rubin, Y., Mavko, G., Harris, J., 1992. Mapping permeability in heterogeneous aquifers using hydrologic and seismic data. Water Resources Research 28 (7), 1809–1816.
Shlomi, S., Michalak, A.M., 2007. A geostatistical framework for incorporating transport information in estimating the distribution of a groundwater contaminant plume. Water Resources Research 43 (3), W03412.
Slater, L., 2007. Near surface electrical characterization of hydraulic conductivity: From petrophysical properties to aquifer geometries—a review. Surveys in Geophysics 28 (2–3), 169–197.
Stone, C.J., 1996. A course in probability and statistics. Duxbury Press, Boston (828 pp.).
Wong, P.-Z., Koplik, J., Tomanic, J.P., 1984. Conductivity and permeability of rocks. Physical Review B 30 (11), 6606–6614.
Wood, G.H., Kehn, T.M., Carter, M.D., Culbertson, W.C., 2003. Coal resource classification system of the U.S. Geological Survey. U.S. Department of the Interior 7.
Zimmerman, D.A., et al., 1998. A comparison of seven geostatistically based inverse approaches to estimate transmissivities for modeling advective transport by groundwater flow. Water Resources Research 34 (6), 1373–1413.